

Comparative Experimental Validation of Human Gait Tracking Algorithms for an Intelligent Robotic Rollator

Georgia Chalvatzaki, Xanthi S. Papageorgiou, Costas S. Tzafestas and Petros Maragos
School of Electrical and Computer Engineering, National Technical University of Athens, Greece
{gchal, xpapag}@mail.ntua.gr, {ktzaf, maragos}@cs.ntua.gr

Abstract—Tracking human gait accurately and robustly constitutes a key factor for a smart robotic walker, aiming to provide assistance to patients with different mobility impairment. A context-aware assistive robot needs constant knowledge of the user’s kinematic state to assess the gait status and adjust its movement properly to provide optimal assistance. In this work, we experimentally validate the performance of two gait tracking algorithms using data from elderly patients; the first algorithm employs a Kalman Filter (KF), while the second one tracks the user legs separately using two probabilistically associated Particle Filters (PFs). The algorithms are compared according to their accuracy and robustness, using data captured from real experiments, where elderly subjects performed specific walking scenarios with physical assistance from a prototype Robotic Rollator. Sensorial data were provided by a laser rangefinder mounted on the robotic platform recording the movement of the user’s legs. The accuracy of the proposed algorithms is analysed and validated with respect to ground truth data provided by a Motion Capture system tracking a set of visual markers worn by the patients. The robustness of the two tracking algorithms is also analysed comparatively in a complex maneuvering scenario. Current experimental findings demonstrate the superior performance of the PFs in difficult cases of occlusions and clutter, where KF tracking often fails.

I. INTRODUCTION

Older adults face various mobility problems, as they have to cope with instability and lower gait speed. Changes in stride length and walking phases are connected to certain pathologies, [1]. Elder care constitutes a major issue for modern societies. Robotics seems to fit naturally to the role of assistance, as it can incorporate features such as posture support and stability, walking assistance and medical monitoring.

Our aim is to use intelligent robotic platforms (Fig. 1), which can monitor and understand the patient’s walking state and reason autonomously on performing assistive actions regarding the patient’s mobility and ambulation, [2]. We are working on the development of an Adaptive Context-Aware Robot Control Architecture (ACARCA), when the robotic assistant is in front of the user, either on supporting or following mode, and detects the patient’s mobility state by using real-time data from sensors mounted on the robotic platform. We can estimate gait parameters and also recognize specific gait patterns, indicating particular pathologies in a non-invasive way, [3]. The user’s gait parameters are necessary to

This research work has been partially supported by the European Union under grant agreement no. 600796 (FP7-ICT-2011-9 2.1, MOBOT Project) and grant agreement no. 643666 (H2020-PHC-19-2014, I-SUPPORT).

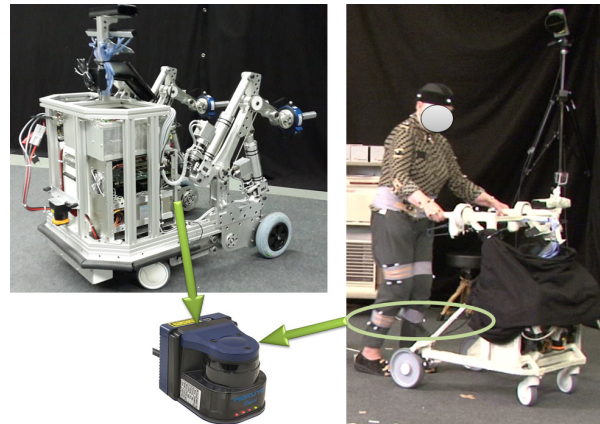


Fig. 1: Left: MOBOT robotic platform equipped with a Hokuyo LRF for recording the user’s gait data (below knee level). Right: Snapshot of a subject walking with physical support of MOBOT.

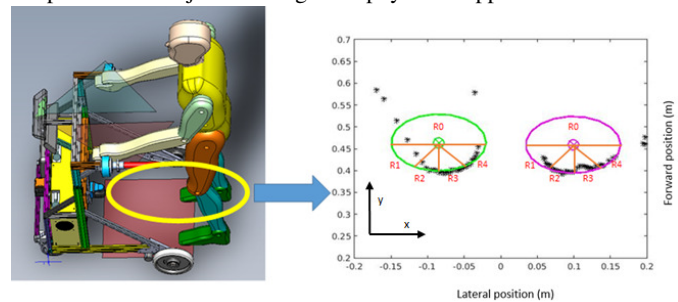


Fig. 2: Example of the legs’ planar representation w.r.t. the LRF. Left: a CAD presentation of a subject walking with the rollator; Right: black stars are the laser points, green and magenta lines are the the right and left leg circular appearances respectively; the orange lines are the regions for the particles’ observation likelihood.

the ACARCA, since it will trigger control assistive actions and behaviors (velocity adjustment, approach of the patient due to changes in gait status) from the robotic assistant. Thus, it is crucial to have a robust tracking system, that accurately estimates the kinematic state of the user, [4].

In this paper, we present a validation study of two human gait tracking systems for elderly subjects. The continuous legs tracking is an important module of the robotic assistant platform (Fig. 1), that utilizes data from the laser sensor mounted on the robotic rollator, which neither interferes with human motion nor it demands the subjects to wear special clothing, shoes or wearable sensors. The first approach is based on K-means clustering and KF. The second approach is based on two probabilistically associated PFs

for tracking each leg separately. The results of both methods are experimentally validated using ground truth data from motion markers, that were used during experiments with the Robotic Rollator, Fig. 1. The comparison regards the tracking of the robotic platform’s users while walking in complex environments with obstacles and clutter that require difficult maneuvers. Our goal is to employ this setup as a subsystem within a larger behavior-based robot control framework, that will constantly and accurately track the user, estimate the subject’s kinematic state and assess its pathological status.

Smart walking support devices, [5], aiming to assist the elderly in standing, walking, as well as detecting abnormalities and assessing rehabilitation procedures is a modern research problem. Different sensors have been employed for extracting gait motions, such as foot pressure distributions (Smart Shoes), [6], accelerometers, [7], visual information, [8], etc. Other approaches refer to human detection and tracking, or recognition of human activity utilizing Laser Rangefinder sensors (**LRF**), either complementary with cameras, or force sensors, [9].

Most research work on human detection and tracking exploits data either from static LRFs, as in pedestrian tracking, [10], or from mounted LRFs on mobile robotic platforms for person following, [11], [12] and group detection and tracking, [13]. In [14] legs are detected using a supervised learning method of leg clusters shapes and tracked them using a multiple-hypothesis tracking framework, but the robustness of the method is yet to be proved. In [15] the authors presented a leg tracking scheme for a telepresence mobile robot following people. The legs are detected using geometrical features but no stochastic filter is applied on the detected positions. Approaches of normal gait detection for mobile robots without using stochastic methods can be found in [16], while [17] refers to parkinsonian gait detection using geometrical features. Human-centered tracking with PF using LRFs mounted on mobile robots can be found in [18], [19], while in [20] the researchers performed leg tracking by using two LRFs and PF-based prediction of the legs’ state. [21] presented a human-centered tracking framework utilizing laser data for a mobile robot, where laser points were grouped and classified as human or not. The detected person’s position is tracked using a KF and scan-to-scan data association; the algorithm is not tested with mobility impaired subjects. Human motion modeling and accurate body tracking has been tested using Motion Capture data, [22]. To our best knowledge, there is no current literature on the topic of legs’ tracking validation using motion capture data.

This paper presents a comparative study of two human gait tracking frameworks for a robotic assistant platform for elderly people; the first is based on KF and the second uses two probabilistically associated PFs with a novel observation model, for the estimation of the legs’ positions and velocities of a subject using a robotic assistant platform (Fig. 1). The accurate and continuous gait tracking is crucial for the robotic assistant platform, as it is an input to the low level controller, [23], but it will also contribute to the context-

awareness of the robotic platform. In our previous work, we have shown how the user’s estimated kinematic parameters are fed to an HMM-based pathological gait recognition system, for detecting specific gait phases. Given that segmentation we extract spatiotemporal gait parameters, which will be used for the impairment level assessment of the user in an ACARCA, [3]. Instead of using complex models and motion tracking approaches that require expensive or bulky sensors and recording devices that interrupt human motion, the measured data used in this work are provided by a standard LRF mounted on a robotic rollator platform. In this work, we aim to experimentally validate the performance of the two gait tracking methods by comparing: (i) their accuracy in estimating the kinematic state of the user’s legs w.r.t. ground truth data from visual markers and, (ii) their tracking robustness in complex and cluttered environments that require difficult maneuvers leading to occlusions, where the KF methodology fails to track the user and requires re-initializations, while the PFs perform an efficient estimation of the users’ legs state without needing any algorithmic manipulation.

II. HUMAN LEGS’ TRACKING: KF

The first approach is a recursive system using a KF, [24]. The state vector comprises the Cartesian coordinates of the centroid legs’ positions and their velocities w.r.t the LRF along the axes. We use the standard KF state equations, [25], where the respective matrices are defined in [24]. We model the legs’ motion as dynamic points, with the acceleration being the control input, since it is “user” generated and we do not have any measurements, i.e. we treat the acceleration as process noise having the same statistics throughout the gait.

At each time frame, the raw laser data, are converted from polar to Cartesian coordinates. In preprocessing, we define an observation window, i.e. a rectangle area in the LRF’s scanning plane, where the user is expected to be w.r.t. the rollator. At time frame $k=1$, the observation window is initialized with predefined dimensions; in the consecutive frames it is adjusted according to the uncertainty of the predicted legs’ positions. The laser points lying outside the window are discarded, while the remaining are separated into groups according to thresholding criteria; laser points outside of the window are discarded, while the remaining are separated into groups. If any laser group contains less than a specific number of points, it is deleted. We wish to end up with two groups, which are labeled as left/right leg by the K-means clustering algorithm. Legs’ centers are computed via circle fitting, and form the observation vector for the KF. Cases in which either one leg is occluded by the other or there is environmental clutter, can interrupt or contaminate the detection. To address such cases of detection loss while continuing the leg tracking, an only-prediction KF is applied; i.e. we perform only the prediction step. If detection loss occurs for a pre-specified number of consecutive frames, we re-initialize the algorithm.

III. HUMAN LEGS' TRACKING: PFS

The PF is commonly used for nonlinear filtering problems, [26]. Our implementation incorporates two filters for estimating the position and velocity of each leg separately and associates them probabilistically. The particles represent samples of the posterior density distribution of the legs' states \mathbf{x}_k^{left} and \mathbf{x}_k^{right} at each time instant k for the left and right leg, respectively. We follow the common algorithmic approach for PFS:

A. Initialization: At time instant $k=1$, we initialize a set of N particles for each leg. Let the position of the i^{th} particle, for $i = 1, \dots, N$, be noted as: $\mathbf{p}_k^{f,i} = [x \ y]^T$ and its velocity as: $\mathbf{v}_k^{f,i} = [v_x \ v_y]^T$, where $f \in \{left, right\}$ is the label of each leg. The particles' states are denoted as: $\mathbf{x}_k^{f,i} = [\mathbf{p}_k^{f,i} \ \mathbf{v}_k^{f,i}]^T = [x \ y \ v_x \ v_y]^T$. Only for initialization, we implement the detection phase described previously in Section II, to detect the legs' positions w.r.t. the LRF and label them as left/right leg. The particles' positions are initialized to be equal to the detected positions. We also draw N samples for the legs' velocity from a zero-mean Gaussian Mixture Model (**GMM**) distribution (we consider that both legs are still in front of the rollator for initialization). The particles' weights $\omega_k^{f,i}$ of each leg are initialized equal to: $1/N$, with $i = 1, \dots, N$. The initial posterior estimate of each leg is approximated by the Minimum Mean Square Error: $\mathbf{x}_k^f = \sum_{i=1}^N \omega_k^{f,i} \cdot \mathbf{x}_k^{f,i} = [\mathbf{p}_k^f \ \mathbf{v}_k^f]^T$.

B. Particles' Propagation: In the next frames $k=2, \dots, T$ (T is the total tracking time), the particles' states are propagated in time using the following motion model. We draw N new velocity samples for the particles of each leg from a GMM of two mixtures. We have trained two GMMs that describe the velocity of the two legs along the axes. Let $\mathbf{v}_k^{f,i}$ be the i^{th} velocity sample drawn from the respective GMM at time instant k . Then, the position of the i^{th} particle is propagated in time according to the equation: $\mathbf{p}_k^{f,i} = \mathbf{p}_{k-1}^{f,i} + \mathbf{v}_k^{f,i} \cdot \Delta t$, where $\mathbf{p}_{k-1}^{f,i}$ is the estimated position vector of each leg for the $k-1$ time frame.

C. Particles' Weights Update: The weights are updated according to the observations of each time instant k . The observations are the Cartesian positions of the laser points in the sagittal plane. In this implementation, we use an observation window for each leg, which is an experimentally defined rectangular area, centered around each particle, so that every sample $\mathbf{x}_k^{f,i}$ is associated with a different cluster of laser points, $\mathbf{y}_k^{f,i}$. Because the prior is equal to the proposal distribution, the weights are equal to the observation likelihood, [26]: $\omega_k^{f,i} = p(\mathbf{y}_k^{f,i} | \mathbf{x}_k^{f,i})$. We treat each particle as a possible leg center and we expect the observations to be on the circular circumference of this center. Thus, the observation likelihood is computed based on three factors:

1. The distribution of the laser points in the circular contour given the center (i.e. the respective particle): In Fig. 2 an example of the legs' circular representation from the laser points w.r.t. the laser scanner is presented. On the right of Fig. 2, we present the detected laser points with black

stars, while the green and magenta circles are the circular representations of the right and left leg, respectively. The labels $R0, R1, R2, R3, R4$ denote the segmentation of the circle into regions (the regions' boundaries are depicted with orange lines) based on which we compute the observation likelihood for the PF tracking system. We have divided horizontally the circle into two semicircles. Laser points in the upper semicircle $R0$ do not contribute to the observation likelihood. The lower semicircle is split into *four* regions ($R1, \dots, R4$) of equal angle range. We have calculated the normal distribution of the Euclidean distances of the laser points of each region w.r.t. the corresponding center. Let \mathbf{d}_{R_m} be the vector of distances of the laser points w.r.t. the corresponding circle center for the R_m region, with $m = 1, \dots, 4$. The points of each R_m are associated with a normal distribution of the distances $\mathcal{N}(\mathbf{d}_{R_m} | \mu_{R_m}, \Sigma_{R_m})$, with μ_{R_m} the mean distance and Σ_{R_m} is the covariance matrix.

2. The number of laser points inside each observation window: Through experimentation we have defined a normal kernel distribution λ_i for every particle with $i = 1, \dots, N$, describing the likelihood of the number of laser points that are detected on the leg's circular contour.

3. An association probability that accounts the Euclidean distance between the two legs. The human legs are two interacting moving targets, and thus we introduce an association probability β_i , modeled by a Gamma distribution. This probability regulates the observation likelihood of the one leg w.r.t. the other, by evaluating a likelihood of the Euclidean distance of the two legs.

We consider the i^{th} particle to be a possible leg center and we compute the observation likelihood using the following function: $p(\mathbf{y}_k^{f,i} | \mathbf{x}_k^{f,i}) = \beta_i \cdot \left[\lambda_i \cdot \sum_{m=1}^4 \pi_{R_m} \cdot \mathcal{N}(\mathbf{d}_{R_m} | \mu_{R_m}, \Sigma_{R_m}) \right]$. We assume as π_{R_m} the importance weights of the four regions, which were set experimentally so that the extreme regions $R1$ and $R4$, often containing many outliers, have less importance than the inner regions $R2$ and $R3$. All parameters have been experimentally defined. The i^{th} weight is equal to: $\omega_k^{f,i} = p(\mathbf{y}_k^{f,i} | \mathbf{x}_k^{f,i})$. All weights are normalized for all particles $j = 1, \dots, N$ according to: $\hat{\omega}_k^{f,i} = \omega_k^{f,i} / \sum_{j=1}^N \omega_k^{f,j}$.

D. Resampling: It commonly occurs many particles to have infinitely small weights and only a few of them will have a significant weight, called weight degeneracy. The solution to this problem is the use of a Sequential Importance Resampling method [26], for eliminating small weighted particles and replace them with higher weighted ones. However, this resampling method illustrates the impoverishment problem, where there are many replicates of the higher-likelihood particles, causing a diversity loss. Thus, at each time frame we check whether the effective sampling size $N_{eff} = 1 / \sum_{i=1}^N \hat{\omega}_k^{f,i}$ is less than the threshold $N_{thr} = N/2$. If so, we apply a random walk on the current particles' state providing new samples $\mathbf{x}_k^{f,i}$; we evaluate the new weights, according to the Particles' Weights Update method: $\hat{\omega}_k^{f,i}$. Having the old pairs of particles and their weights

$(\mathbf{x}_k^{f,i}, \hat{\omega}_k^{f,i})$ along with the new ones $(*\mathbf{x}_k^{f,i}, *\hat{\omega}_k^{f,i})$, we apply the Metropolis-Hastings algorithm, [27], to decide whether or not we have to replace the i^{th} pair $(\mathbf{x}_k^{f,i}, \hat{\omega}_k^{f,i})$ with the new samples $(*\mathbf{x}_k^{f,i}, *\hat{\omega}_k^{f,i})$.

E. Posterior Estimation: For the posterior state estimate $p(\mathbf{x}_k^f | \mathbf{y}_k^f)$, we find the particle with the highest weight and then collect the “best” particles, i.e. those having a weight greater or equal than 80% of the maximum weight: $S = \arg \max_i [\hat{\omega}_k^{f,i} \geq 0,8 \cdot \max(\hat{\omega}_k^{f,i})]$, where $S \subseteq \{1, \dots, N\}$ is the set of the “best” particles. In that way, we have a dynamic system that provides smoother estimates, by leaving out particles that may track outliers and could contaminate the posterior estimation. The posterior state estimate is then approximated by the weighted mean of the “best” particles, with $s \in S$ being the index of the “best” particles: $p(\mathbf{x}_k^f | \mathbf{y}_k^f) = \left(\sum_s \mathbf{x}_k^{f,s} \cdot \hat{\omega}_k^{f,s} \right) / \left(\sum_s \hat{\omega}_k^{f,s} \right)$.

IV. EXPERIMENTAL ANALYSIS & VALIDATION

A. Experimental setup and data description

The experimental data used in this work were collected in Agaplesion Bethanien Hospital - Geriatric Center with the participation of real patients, under ethical approval by the ethics committee of the Medical Department of the University of Heidelberg. All subjects had signed written consent for participating in the experiments. The participants presented moderate to mild mobility impairment, according to clinical evaluation. The patients were wearing their normal clothes. A set of motion markers from a VICON Motion Capture system was placed on certain areas of the subjects’ body. A Hokuyo UBG-04LX-F01 rapid LRF was mounted on the robotic platform of Fig. 1 for the detection of the patients’ legs. The LRF is placed at a height of about 40 cm from the ground in order to capture tibia motion.

In this work, we present results for four patients aged over 65 years old. The subjects participated in two walking scenarios, performing each of them twice; **Scenario 1**: the subjects walked with physical support of the rollator on a straight direction of about 3 m, performed a 180° turn and returned to initial position. **Scenario 2**: the subjects, walking with physical support of the rollator, performed a richer scenario, where they had to make turning maneuvers at the middle of the walkway to avoid obstacles. All patients performed the experimental scenarios under appropriate carer’s supervision. The subjects were instructed to walk as normally as possible. A snapshot of the experimentation scene with a subject walking supported by the robotic rollator while wearing a set of visual markers is shown on the left of Fig. 3; on the right, a representation of the markers from the MOKKA visualization system is provided. Marked with green are the Tibia markers and with red the Rollator markers, which are used in this work, for the validation study.

B. Validation Strategy

Our validation strategy comprises the comparison of the two gait tracking algorithms regarding their accuracy and robustness. For the accuracy testing, we validate the results

TABLE I: Tracking Accuracy

Scenario 1						
Subject	Parameter	Unit	RMSE		MAD	
			KF	PF	KF	PF
1	x	cm	9.73	2.65	5.63	1.72
	y	cm	16.36	4.32	10.87	2.48
	v _x	cm/s	10.44	6.91	6.81	4.69
	v _y	cm/s	31.98	15.93	21.59	11.23
2	x	cm	2.62	2.35	1.17	0.86
	y	cm	4.58	3.82	3.07	1.22
	v _x	cm/s	5.28	4.54	3.88	3.46
	v _y	cm/s	16.09	12.57	12.25	9.39
3	x	cm	9.36	4.57	6.15	2.84
	y	cm	8.73	6.20	5.13	3.59
	v _x	cm/s	4.53	4.20	3.37	2.93
	v _y	cm/s	10.89	7.06	7.95	5.07
4	x	cm	6.19	4.40	4.85	2.91
	y	cm	9.52	6.78	8.41	4.34
	v _x	cm/s	11.34	9.86	8.03	7.66
	v _y	cm/s	28.41	20.22	20.83	15.32
Scenario 2						
Subject	Parameter	Unit	RMSE		MAD	
			KF	PF	KF	PF
1	x	cm	8.14	2.83	7.35	1.54
	y	cm	10.29	4.16	7.53	1.94
	v _x	cm/s	10.21	7.00	7.65	4.67
	v _y	cm/s	16.05	13.30	23.09	9.69
2	x	cm	3.88	3.59	2.46	1.91
	y	cm	6.55	5.21	4.13	3.24
	v _x	cm/s	6.94	6.52	4.93	4.81
	v _y	cm/s	18.09	11.23	13.33	8.47
3	x	cm	2.55	2.50	2.17	1.23
	y	cm	4.48	4.96	3.76	1.78
	v _x	cm/s	6.61	6.47	5.11	4.90
	v _y	cm/s	14.33	13.14	10.97	10.15
4	x	cm	3.89	3.58	2.72	1.72
	y	cm	7.72	5.58	5.08	1.93
	v _x	cm/s	10.85	9.06	7.70	6.81
	v _y	cm/s	20.77	15.64	13.73	11.20

Statistical comparison of the two filters using the average RMSE and the MAD error.

TABLE II: Tracking Robustness

Scenario 1					
Subject		Total Tracking time (s)	Total errors (# frames)	Total errors (% of total frames)	# Re-initialization
	PF	56.16	0	0	-
2	KF	113.56	384	10.5	288
	PF	124.04	107	2.3	-
3	KF	65.93	1049	30.1	1473
	PF	94.26	0	0	-
4	KF	44.12	272	14.3	95
	PF	51.46	0	0	-
Scenario 2					
1	KF	86.21	2095	39.6	1930
	PF	142.78	0	0	-
2	KF	88.34	445	11.8	72
	PF	101.44	0	0	-
3	KF	69.49	0	0	0
	PF	69.49	0	0	-
4	KF	84.81	41	1.3	27
	PF	85.91	0	0	-

Total tracking time and tracking errors for all subjects for evaluating the tracking robustness of the two filters.

of the filters with the ground truth data by comparing their average Root Mean Square Errors (**RMSE**) and average Mean Absolute Deviation (**MAD**) of the errors over the total tracking time. As ground truth data, we have isolated the raw data from the markers placed on the Tibia and the Robotic rollator, Fig. 3. We applied interpolation and smoothing on the markers trajectories and performed cylin-

der fitting on the tibia markers for representing the user's tibia at each time frame. We subtracted the cylinder's points that corresponded to the field of view of the LRF. Using the rollator markers' data, we have applied a Euclidean transformation on the data to project them to the LRF's reference frame. The legs' velocities resulted from simple differentiation. The robustness of the filters refers to the successful tracking time, tracking errors, re-initialization times, etc., as well as graphical depiction of tracking results in difficult cases (occlusion/clutter). The noise parameters of the KF are: regarding the process noise affected by the acceleration variability: $\sigma_{a_x^L} = 1.63(m/s^2)$, $\sigma_{a_y^L} = 5.24(m/s^2)$, $\sigma_{a_x^R} = 1.63(m/s^2)$, $\sigma_{a_y^R} = 5.24(m/s^2)$; and the measurement noise variance, accounting the LRF's nominal noise and the variability in the circle fitting: $v_{x_k} = 0.059(m)$ and $v_{y_k} = 0.02(m)$, [24]. The PF implementation was tested with 500 particles per leg.

C. Validation Results and Discussion

1) *Accuracy*: Table I contains the statistics for the average RMSE and MAD of the tracking algorithms estimations w.r.t. ground truth data. The parameters x, y refer to the mean position and v_x, v_y to the mean velocity of both legs. We can see that the PF tracking algorithm has better performance than the KF implementation both in Scenario 1 and in the more complex Scenario 2 (with bold font are noted the lower RMSE and MAD values). The average precision increase by using the PF algorithm instead of KF, corresponds to approximately 30% RMSE and 43% MAD error reduction. The relatively higher errors in velocity estimation can be partially explained by the way the ground truth velocity is computed (simple differentiation of markers' positions) that induces random noise. Also, the cylinder fitting supposes that the legs have an even surface, while the laser clusters are highly deformable due to users' clothing. An example of the tracking algorithms for the estimation of the left and right lateral (Fig. 4a, 4b) and forward positions (Fig. 4c, 4d) of subject #1 in Scenario 2 is presented in Fig. 4. The black lines represent the KF estimates, the blue lines the PF estimates and the red lines the ground truth. The KF fails to track the position of the user, thus explaining the high errors of subject #1 in Scenario 2, Table I, while the PF tracks the user quite accurately (Table I lower RMSE and MAD).

2) *Robustness*: The evaluation of the filters' tracking robustness is based on Fig. 5. The black stars represent the raw laser data. On the left, the red "x" is the left KF estimated and the green "x" the left detected leg position, while the blue "x" is the right KF estimated and the magenta "x" the right detected leg position. On the right, the green circles are the left leg particles and the red "x" is its PF position estimate, while the magenta circles are the right leg particles and the blue "x" is its PF estimation. In Fig. 5a, Fig. 5b a comparison of a typical case of cluttered environment is shown, for which the KF wrongly estimates the position of the two legs by detecting a "leg" on the noisy background, while the PF performs well in detecting the position of the two legs regardless of the clutter. In Fig. 5c, Fig. 5d

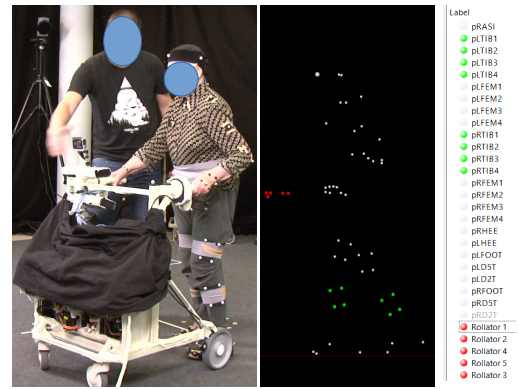


Fig. 3: Left: Snapshot from the experimentation scene. A patient wears a set of visual markers while walking with the robotic assistant rollator. Right: a representation of the visual markers from MOKKA visualization system. We are interested in the Tibia markers (green) and the rollator markers (red).

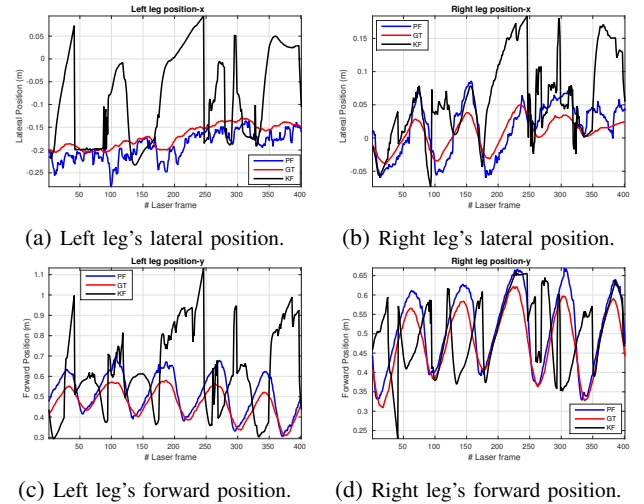


Fig. 4: Example of the estimated positions and the ground truth data. Black line: KF estimate, blue line: PF estimate, red line: ground truth (forward and lateral directions are shown in Fig. 2).

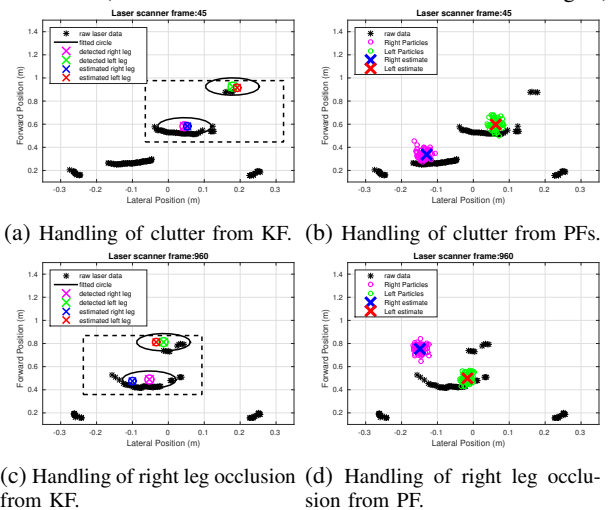


Fig. 5: Comparison of clutter (a, b) and occlusion (c, d) problems by the two tracking algorithms.

we present the handling of a leg occlusion case, where the PFs predict the occluded right leg's position, while the

KF-based algorithm fails to predict the left leg's position, causing a false estimation for the occluded leg. The proposed computation of the observation likelihood for the PF tracker with the data association gives better results than the KF tracker, in cases of great noise, e.g. due to clothing, where the KF tracking system fails most of the times to correctly estimate the leg centers, while the PF observation likelihood penalizes points that seem to be outliers.

Table II presents the total time of correct tracking, the total tracking errors both in frames and as a percentage of the total frames provided by the LRF. It also contains the re-initialization times of the KF tracking algorithm. The PF tracks almost all users successfully.

Only for subject #2 in Scenario 1, PF has a 2.3% false tracking, but it was due to the wrong initialization of the filter because of the cluttered environment; however the particles in our implementation had the necessary variability to dynamically search and finally get assigned correctly to the user's legs; therefore the PF-based tracking manages to detect and track the user successfully for the rest of the scenario without using any re-initializations of the algorithm. The KF algorithm achieves successful tracking only for subject #3 in Scenario 2. The highest tracking error occurs in subject #1 during the complex walking Scenario 2 with a failure percentage of 39.6% of the total frames. The KF algorithm tracks the user successfully in straight paths, but almost always loses track of the user in turns when the legs are occluded and requires re-initialization; without it, the filter does not manage to re-detect the user and loses track of him.

V. CONCLUSIONS AND FUTURE WORK

For a completely non-invasive pathological walking analysis and assessment system in a context-aware robot control for an intelligent robotic walker, the accurate and robust tracking system of the user's legs is a crucial parameter. We utilize data from an LRF mounted on a robotic assistant platform, constituting a non-invasive approach using a non-wearable device. We validate the performance of two human gait tracking algorithms; a system based on KF and a second one based on two probabilistically associated PFs. The two methodologies are compared regarding their accuracy in estimating the user's legs kinematic state with ground truth data from visual markers, worn by patients while walking with the assistant robot in real experimental scenarios. The robustness of the two tracking algorithms is also examined. The experimental results clearly present the superiority of the PFs over the KF system. The PF methodology is more accurate in estimating the user's kinematic state, and it can also successfully handle difficult cases of leg occlusions and clutter and can track patients with different mobility inabilities, while they are walking in mazy environments needing complex maneuvers, when the KF fails.

Our goal is to develop a multilayered PF tracking system for an augmented state estimation of the user. We aim to implement a multiple motion model PF tracker for a real time estimation of gait parameters, that will provide feedback for an ACARCA. We intend to create a system for detecting

in real time specific gait pathologies and automatically classify the patient status or the rehabilitation progress, thus providing the necessary information for effective cognitive active mobility assistance robots.

REFERENCES

- [1] J. M. Hausdorff, "Gait dynamics, fractals and falls: Finding meaning in the stride-to-stride fluctuations of human walking," *Human Movement Science* 2007.
- [2] X. Papageorgiou et. al., "Advances in intelligent mobility assistance robot integrating multimodal sensory processing," *Lecture Notes in Computer Science, Universal Access in Human-Computer Interaction, Aging and Assistive Environments*, 2014.
- [3] X. Papageorgiou et. al., "Experimental validation of human pathological gait analysis for an assisted living intelligent robotic walker," in *Biorob* 2016.
- [4] G. Chalvatzaki et. al., "Experimental comparison of human gait tracking algorithms: Towards a context-aware mobility assistance robotic walker," in *MED* 2016.
- [5] M. Spenko et. al., "Robotic personal aids for mobility and monitoring for the elderly," *IEEE Trans. on Neural Systems and Rehabilitation Engineering*, 2006.
- [6] J. Bae and M. Tomizuka, "Gait phase analysis based on a hidden markov model," *Mechatronics*, 2011.
- [7] C. Nickel et. al., "Using hidden markov models for accelerometer-based biometric gait recognition," in *CSPA* 2011.
- [8] G. e. Bebis, "An architecture for understanding intent using a novel hidden markov formulation," *Int'l J. of Humanoid Robotics*, 2008.
- [9] A. Panagadan et. al., "Tracking and modeling of human activity using laser rangefinders," *Int'l Journal of Social Robotics*, 2010.
- [10] F. M. Chang et. al., "Integration of modified inverse observation model and multiple hypothesis tracking for detecting and tracking humans," *IEEE Trans. on Automation Science and Engineering*, 2016.
- [11] T. Horiuchi et. al., "Pedestrian tracking from a mobile robot using a laser range finder," in *ISIC* 2007.
- [12] K. Arras et.al., "Efficient people tracking in laser range data using a multi-hypothesis leg-tracker with adaptive occlusion probabilities," *ICRA*, 2008.
- [13] T. Linder et. al., "On multi-modal people tracking from mobile platforms in very crowded and dynamic environments," in *ICRA* 2016.
- [14] K. Arras et. al., *Range-Based People Detection and Tracking for Socially Enabled Service Robots*. Springer Berlin Heidelberg, 2012.
- [15] A. Cosgun et. al., "Autonomous person following for telepresence robots," in *ICRA* 2013.
- [16] H. Kim et. al., "Detection and tracking of human legs for a mobile service robot," in *AIM* 2010.
- [17] W.-H. Mou et. al., "Context-aware assisted interactive robotic walker for parkinson's disease patients," in *IROS* 2012.
- [18] N. Belloto and H. Hu, "People tracking with a mobile robot: A comparison of kalman and particle filters." *IASTED* 2007.
- [19] P. Chakravarty et. al., "Panoramic vision and laser range finder fusion for multiple person tracking," in *IROS* 2006.
- [20] T. Ohnuma et. al., "Particle filter based lower limb prediction and motion control for jaist active robotic walker," in *2014 RO-MAN*.
- [21] A. Leigh et. al., "Person tracking and following with 2d laser scanners," in *ICRA* 2015.
- [22] C. Prakash et. al., "Identification of spatio-temporal and kinematics parameters for 2-d optical gait analysis system using passive markers," in *ICACEA* 2015, 2015.
- [23] G. Chalvatzaki et. al., "Gait modelling for a context-aware user-adaptive robotic assistant platform," in *IMAACA* 2015.
- [24] X. Papageorgiou et. al., "Hidden markov modeling of human pathological gait using laser range finder for an assisted living intelligent robotic walker," in *IROS* 2015.
- [25] Y. Bar-Shalom and X.-R. Li, "Estimation and tracking: Principles, techniques, and software [reviews and abstracts]," *IEEE Antennas and Propagation Magazine*, 1996.
- [26] M. Arulampalam et. al., "A tutorial on particle filters for online nonlinear/non-gaussian bayesian tracking," *IEEE Trans. Signal Processing*, 2002.
- [27] Z. Chen, "Bayesian Filtering: From Kalman Filters to Particle Filters, and Beyond," McMaster University, Tech. Rep., 2003.